First posted online on 25 May 2018 as 10.1242/dev.159657
Access the most recent version at http://dev.biologists.org/lookup/doi/10.1242/dev.159657

miR-133 mediated regulation of the Hedgehog pathway orchestrates embryo myogenesis

Gi Fay Mok[1], Estefania Lozano-Velasco[1,$], Eirini Maniou[1,$], Camille Viaut[1,3,$], Simon Moxon[2,4], Grant Wheeler[1] and Andrea Münsterberg[1,*]

[1] School of Biological Sciences, Cell and Developmental Biology, University of East Anglia, Norwich Research Park, Norwich, NR4 7TJ, UK

[2] The Earlham Institute, Norwich Research Park Innovation Centre, Colney Lane, Norwich NR4 7UH, UK

[3] Present address: INSERM U1016, CNRS UMR8104, Institut Cochin, Université Paris Descartes, Department of Development, Reproduction and Cancer, 24 Rue du Faubourg St Jacques, Paris 75014, France

[4] Present address: School of Biological Sciences, University of East Anglia, Norwich Research Park, Norwich, NR4 7TJ, UK

[$] These authors contributed equally and are listed alphabetically

*Corresponding author:

Email: a.munsterberg@uea.ac.uk

Phone: +441603592232

ABSTRACT

Skeletal myogenesis serves as a paradigm to investigate the molecular mechanisms underlying exquisitely regulated cell fate decisions in developing embryos. The evolutionary conserved miR-133 family of microRNAs is expressed in the myogenic lineage, but how it acts remains incompletely understood. Here we performed genome-wide differential transcriptomics of miR-133 knock-down (KD) embryonic somites, the source of vertebrate skeletal muscle. This revealed extensive downregulation of Sonic hedgehog (Shh) pathway components: patched receptors, Hedgehog interacting protein, and the transcriptional activator, Gli1. By contrast Gli3, a transcriptional repressor, was de-repressed and confirmed as a direct miR-133 target. Phenotypically, miR-133 KD impaired myotome formation and growth by disrupting proliferation, extracellular matrix deposition and epithelialization. Together this suggests that miR-133 mediated Gli3 silencing is critical for embryonic myogenesis. Consistent with this idea we found that activation of Shh signalling by either purmorphamine, or KD of Gli3 by antisense morpholino (MO) rescued the miR-133 KD phenotype. We identify a novel Shh/MRF/miR-133/Gli3 axis that connects epithelial morphogenesis with myogenic fate specification.

Keywords: miR-133, chick embryo, somite myogenesis, Sonic hedgehog signalling, Gli3, basement membrane

INTRODUCTION

Skeletal muscle is important for mobility and survival. Its development is a highly regulated process, involving developmental signals and their effector pathways, a hierarchy of transcription factors – the myogenic regulatory factors (MRFs) and post-transcriptional regulation by non-coding RNAs (Buckingham and Rigby, 2014; Mok and Sweetman, 2011).

In vertebrate embryos, skeletal muscles of the trunk and limbs are derived from somites, transient paired segments that form in a regular sequence on either side of the neural tube and notochord (Christ and Scaal, 2008). In response to signals, including Wnt, Shh and Notch (Abou-Elhamd et al., 2015; Abu-Elmagd et al., 2010; Borycki et al., 1999; Johnson et al., 1994; Munsterberg et al., 1995; Rios et al., 2011; Sieiro et al., 2016), the initially epithelial somite undergoes morphogenetic changes and differentiates. On the ventral side, cells dissociate to form the sclerotome, whilst the dermomyotome on the dorsal side remains epithelial and contributes myocyte progenitors to the myotome. Myotome formation initiates at the epaxial lip of the dermomyotome, abutting the neural tube (Gros et al., 2004). Interactions with migrating neural crest cells triggers translocation of dermomyotomal lip progenitors into the myotome, where they orientate, elongate and begin to differentiate into myocytes (Rios et al., 2011; Sieiro et al., 2016).

Shh, derived from the notochord and floor plate, activates myogenesis (Munsterberg et al., 1995), and is essential for the activation of the myogenic determination gene, Myf5, in epaxial muscle progenitor cells in mice (Borycki et al., 1999; Gustafsson et al., 2002), or in both epaxial and hypaxial domains in avian embryos (Kahane et al., 2013). Myf5 activation is mediated via Gli activator proteins, Gli1 and Gli2, acting on a Gli-binding site in the mouse epaxial enhancer (Gustafsson et al., 2002; McDermott et al., 2005; Teboul et al., 2002). In the absence of Shh, the Gli3 repressor inhibits Myf5 transcription (McDermott et al., 2005). Furthermore, in both avian and mouse embryos, Shh signalling is crucial for the transition from proliferating Pax7-positive progenitors to terminally differentiating myocytes (Kahane et al., 2013).

MicroRNAs (miRNAs or miRs) are short noncoding RNAs that bind to target sites located in 3'UTRs of mRNAs. This interaction leads to inhibition of translation, mRNA cleavage and transcript degradation via deadenylation (Bartel, 2009; Bethune et al., 2012). Through their effects on target gene expression, miRNAs regulate developmental timing and provide robustness to cell fate decisions (Ebert and Sharp, 2012; Hornstein and Shomron, 2006). The miR-1/miR-206 and miR-133 families, comprising miR-1-1/miR-1-2/miR-206 and miR-133a/miR-133b are encoded by three loci in mouse and human and by four loci in chicken (Sweetman et al., 2008). One member of each family is produced from the same primary transcripts and they play important roles in regulating proliferation, differentiation and cell fate specification in developing muscle (Horak et al., 2016; Mok et al., 2017). In mouse and chicken embryos, miR-1/miR-133a are expressed in skeletal and cardiac muscle. In contrast, miR-206/miR-133b are expressed in myoblasts of somites, limb buds, and head muscles but not in cardiomyocytes (Darnell et al., 2006; Sweetman et al., 2008). In *Xenopus* and zebrafish the miR-1/miR-206 and miR-133 families are present in skeletal muscle but not detected in the heart (Ahmed et al., 2015; Mishima et al., 2009). Together with myocyte enhancer factor-2 (MEF2) the MRFs regulate expression of miR-1, miR-206 and miR-133, in somites (Liu et al., 2007; Sweetman et al., 2008) and in C2C12 myoblasts (Rao et al., 2006; Rosenberg et al., 2006). In C2C12 myoblasts the miR-1/miR-206 and miR-133 families regulate the balance between differentiation and proliferation through interactions with multiple targets (Alteri et al., 2013; Chen et al., 2006; Feng et al., 2013; Goljanek-Whysall et al., 2012)

We previously used miRNA knock-down (KD) in chick somites to show that miR-1/miR-206 and miR-133 negatively regulate BRG1/BRM-Associated Factor 60 (BAF60) variants BAF60A and BAF60B. This facilitates the preferential incorporation of BAF60C into the BAF/BRG1 chromatin-remodelling complex, required for myogenesis (Goljanek-Whysall et al., 2014). In earlier somites, miR-206 facilitates the complete downregulation of Pax3 in the myotome, ensuring timely transition of myogenic progenitor to committed myoblast (Goljanek-Whysall et al., 2011). Studies in mice showed that miR-133a isoforms are essential for the maintenance of skeletal muscle structure and myofibre identity (Liu et al., 2011), and controlling brown fat differentiation through targeting Prdm16 (Trajkovski et al., 2012); although, deletion of the miR-206/133b cluster did not result in skeletal

muscle defects (Boettger et al., 2014). In zebrafish, transcriptomic analysis revealed the importance of miR-1 and miR-133 for sarcomeric actin organisation (Mishima et al., 2009). However, the functions of miR-133 in early myogenesis remain unclear.

Here, we characterize the mechanisms that underlie the embryonic phenotype resulting from antagomir-mediated miR-133 KD in avian somites. Impaired myogenesis was evident from reduced expression of MRFs, reduced cell proliferation and impaired growth of the dermomyotome and myotome, as well as reduced actin accumulation and disorganized basement membrane (BM) deposition. Differential transcriptomics of miR-133 KD somites identified negative effects on Shh pathway components, suggesting a role for miR-133 in modulating Shh signalling. Expression of the Gli3 transcriptional repressor was de-repressed after miR-133 KD and luciferase assays confirmed direct regulation via a functional target site in the Gli3 3'UTR that is complementary to the miR-133 seed sequence. Myotome formation and epithelialization, BM deposition and myogenic differentiation were restored in miR-133 KD somites by concomitant activation of Shh signalling using purmorphamine, a synthetic agonist of the smoothened (Smo) receptor (Sinha and Chen, 2006), or by the concomitant morpholino-mediated knock down of Gli3 repressor. Our data identify a novel Shh/MRF/miR-133/Gli3 axis and show that stabilization of myogenic differentiation and growth of the myotome require the negative regulation of Gli3 by miR-133.

RESULTS

miR-133 is expressed in nascent myoblasts

The spatio-temporal expression of miR-133 was determined by whole mount *in situ* hybridization. In HH-stage 14 chick embryos (Hamburger and Hamilton, 1951) miR-133 was detected in epithelial and in differentiating somites, as well as in the neural tube, brain and anterior notochord (Fig. S1A). In epithelial somites, expression was detected adjacent to the neural tube, where the first myoblasts emerge, and at low levels throughout. The relative expression levels of miR-133 increased as somites matured, and in differentiating somites miR-133 was restricted to the myotome (Fig. S1A, B), as previously reported for older stage embryos (Goljanek-Whysall et al., 2011; Sweetman et al., 2008) .

miR-133 coordinates cell fate acquisition with somite morphogenesis

Somites are severely affected by antagomir-mediated KD of miR-133, with epithelial morphology lost in the dermomyotome and myotome, and Myogenin (Mgn) expression either lost completely (80%) or partially (20%), indicating that by 24 hours myogenesis is compromised (Figs. 1B, 4B, Goljanek-Whysall et al., 2014).

To characterize in more detail the underlying cellular and molecular mechanisms, we established that effects resulting from miR-133 inhibition were first detected after 9 hours. Epithelial somites of HH14/15 embryos injected with FITC-labelled antagomir-133 (AM133) and examined after 6, 9, 12 or 24 hours (Fig. 1A) showed partial loss of Myf5, MyoD (Fig. S2A) and Mgn expression 9 hours after miR-133 KD (Fig. 1B). No phenotype was detected after 6 hours and after 12 and 24 hours phenotypes were more pronounced (Fig. 1B and S2B). Control injections of scrambled antagomir (AMscr) had no effect (Fig. S3A-D). RT-qPCR confirmed significantly reduced abundance of miR-133 in somites after AM133 injection (Fig. 1C), also observed with Northern blots (Goljanek-Whysall et al., 2014). Interestingly AM133 injections of the equivalent, inter-limb level somites at later stages (HH20), when miR-133 is expressed in a more developed myotome, did not lead to myogenic defects (Fig. S2C), suggesting a critical window in younger, less mature somites where miR-133 function is essential.

Pax3 and Pax7 immunostaining on cryosections revealed a reduced dermomyotome size, confirmed by pixel measurements using Fiji/ImageJ, in AM133 injected somites compared to the contralateral non-injected side (HH14/15) (Fig. 2A,B). Phosphor-histone H3 (pH3) staining showed fewer mitotic cells present in the dermomyotome and myotome indicating impaired cell proliferation after miR-133 KD (Fig. 2C). Immunostaining for caspase-3 (Cas3) showed no detectable increase of apoptotic cells (Fig. S2D). AMscr injections did not affect dermomyotome proliferation or size (Fig. S3A-C).

Epithelial organization of the dermomyotome, assessed by actin staining, showed a reduced number of apico-basal orientated dermomyotomal cells. Furthermore, the dermomyotomal lip was poorly defined, had lost its epithelial character and less actin accumulated (Fig. 2D). In addition, discontinuous and disorganized laminin staining suggested that basement membrane (BM)

deposition was impaired and a BM had not fully formed on the basal side of dermomyotome cells or beneath the myotome (Fig. 2D). The BM surrounding the neural tube remained unaffected and AMscr injections did not affect epithelial organisation of the dermomyotome (Fig. S3D).

Inhibition of miR-133 affects Shh pathway components

The discrete molecular and cellular changes observed after 9 hours in the dermomyotome and myotome following AM133 injection culminate in severe impairment of myogenesis by 24 hours (Figs. 1, 2, S2 and S3). Genome-wide differential transcriptomics of AM133 or AMscr injected somites was used to identify the pathways and cellular processes involved (Fig. 3). This was done at 9 hours to capture the earliest events. Hierarchical clustering confirms that AM133 injected somites were more similar to each other than to control somites and identified differentially expressed genes (Fig. 3B). Gene ontology (GO) analysis shows that genes involved in processes relating to cell division were significantly decreased (Fig. 3C), consistent with observations that dermomyotome size and number of mitotic cells were reduced after miR-133 KD.

Amongst the top 50 significantly downregulated differentially expressed (DE) genes were myogenic markers, Myf5 and MyoD, and sclerotome markers, Pax1 and Pax9. Strikingly, several Shh pathway components were also in this group, including patched-1 (Ptch1) and patched-2 (Ptch2) receptors, Hedgehog interacting protein (HHIP) and the transcriptional activator Gli1 (Fig. 3B, D). Thus, we looked for a transcriptional repressor of Shh pathway genes amongst the genes whose relative expression was increased. A strong candidate was Gli3, which was amongst the top 200 de-repressed genes and its expression was significantly increased ($p=0.03$) (Fig. 3D). Gli3 was therefore a putative direct target gene for miR-133. A miR-133 target site identified in its 3'UTR, conserved in human, chimp, mouse, cow and frog, was validated by luciferase reporter assays. Reporter gene expression was inhibited significantly after transfection of miR-133. Introducing mutations into the 8-mer seed sequence of the target site restored reporter gene expression even in presence of miR-133 (Fig. 3E), confirming its importance. A control microRNA had no effect. Furthermore, analysis of Gli3 protein levels by Western blot confirmed a relative increase of the short repressor isoform (Gli3Rep)

in somites, following miR-133 inhibition *in vivo* using AM133 injection compared to control AMscr injected somites (Fig. 3F).

Shh pathway activation rescues miR-133 KD

The finding that Gli3, which acts predominantly as a transcriptional repressor, is a direct target for miR-133 and de-repressed after miR-133 KD (Fig. 3D, F), led us to test whether pharmacological activation of the Shh pathway can rescue the myogenic phenotype. Knock down of miR-133 completely inhibited myogenesis after 24 hours (Fig. 1B, Fig. 4B, Fig. S2B). However, co-injection of AM133 and purmorphamine, an activator of Shh signalling, restored myogenic differentiation, as shown by expression of Mgn (Fig. 4B). To determine whether Gli3 de-repression was critical for the phenotype observed, we knocked down Gli3 expression using morpholinos (MO) and examined whether this could rescue the AM133 induced loss of Mgn. A FITC-labelled Gli3 translation blocking MO was electroporated concomitant with AM133 injection (Fig. 4C, D). Western blots of transfected somites showed that Gli3Rep protein was reduced by Gli3 MO compared to control MO (Fig. S3F). A faint band representing the full-length Gli3 activator (Gli3Act) was present in both samples, consistent with the finding that Gli3Act becomes rapidly degraded (Wen et al., 2010). *In situ* hybridization showed that Gli3 MO restored myogenesis in AM133 treated somites (Fig. 4D), suggesting that miR-133 mediates its effect via negative regulation of Gli3.

Somite organization was improved after treatment with purmorphamine or the concomitant transfection of Gli3 MO together with AM133, however, the somites were smaller (Fig. 4B, D). Thus, we examined the rescue phenotype in more detail, after 9 hours. Pax3 and Pax7 immunostaining showed that, although the dermomyotome was smaller, its epithelial nature was preserved in somites injected with AM133 and purmorphamine (Fig. 5A-D). Fewer mitotic cells were detected by pH3 staining, compared to contralateral somites (Fig. 5C) and this was similar to somites injected with AM133 alone (Fig. 2C). Actin and laminin staining showed that epithelial character and BM deposition was restored around the dermomyotome and myotome (Fig. 5D).

Finally, AM133 co-injection with purmorphamine restored expression levels of differentially expressed hedgehog-pathway genes (Fig. 6A). Somites injected with AMscr, or with AM133 alone, or with AM133 and purmorphamine were examined using RT-qPCR. Expression of Gli1, Gli2, Ptch1, Smo and HHIP was decreased in somites injected with AM133, whereas expression of Gli3 increased, consistent with the differential transcriptomics data. Purmorphamine co-injection with AM133 led to recovery of Shh pathway components compared to somites injected with AM133 alone. The exception was Gli3 expression, which remained de-repressed. This was not unexpected given that miR-133 function was still inhibited by antagomir-133 (Fig. 6A). The relative expression of Pax3 and Pax7 increased, whilst Myf5 and Mgn expression decreased after antagomir-133 injection. Myf5 was also significantly decreased after miR-133 KD in the differential transcriptomics data (Fig. 3B). Co-injection of purmorphamine with AM133 restored expression of pre-myogenic markers, Pax3 and Pax7, to levels comparable to control somites and Myf5 and Mgn levels were also rescued (Fig. 6B). In addition, expression of snail1, a gene associated with epithelial mesenchymal transition (EMT), or gremlin1, a BMP antagonist was rescued by Shh pathway activation (Fig. 6D). However interestingly, genes associated with proliferation, CDC20, CDK1 and FGF8, remained repressed, consistent with fewer pH3 positive cells and smaller somites in presence of AM133, irrespective of the presence of purmorphamine. This suggests that myogenic differentiation and epithelialization are uncoupled from proliferation and that there is differential sensitivity of these processes for GliAct/GliRep balance. Furthermore, there may be additional functions of miR-133, independent of Gli3 targeting and Shh pathway regulation.

DISCUSSION

Despite recent progress, we still do not have a complete understanding of how myogenic progenitor cells, once specified, can stably execute their differentiation program. microRNAs are involved in fine tuning of developmental processes and we use the accessibility of chicken embryos to investigate the function of the miR-133 family *in vivo*, during embryonic myogenesis using antagomir-mediated inhibition, differential transcriptomics and rescue experiments.

Embryonic loss-of-function of miRNAs is often difficult to investigate due to functional redundancy of almost identical mature miRNAs produced from multiple genetic loci, thus making reverse genetic approaches in mice challenging. Observations from mice with genetic deletion of miR-133a-1 and miR-133a-2 family members suggest a role for adult skeletal muscle homeostasis (Liu et al., 2011). In contrast, removal of the miR-206/133b cluster did not reveal essential functions in skeletal muscle differentiation or regeneration (Boettger et al., 2014). The concomitant knockout (KO) of the miR-1-1/133a-2 and miR-1-2/133a-1 clusters, which are expressed in cardiac and skeletal muscle, led to an early cardiac defect (Wystub et al., 2013). However an embryonic skeletal muscle phenotype was not reported in any of these lines, most likely due to expression from unaffected loci. Chick embryos offer the opportunity to perform conditional miRNA KD experiments using antagomirs that simultaneously inhibit the mature form of all miR-133 family members produced (Goljanek-Whysall et al., 2014). This has uncovered a critical function of miR-133 in the modulation of Shh signalling through direct targeting of Gli3, a transcriptional repressor of the pathway and of myogenesis (McDermott et al., 2005; Wen et al., 2010).

Shh signals, derived from the notochord and floorplate, activate myogenesis in explants of presegmented mesoderm and act on myogenic progenitors in the dermomyotome and dermomyotome lip (Borycki et al., 1999; Borycki et al., 1998; Munsterberg et al., 1995). This induces expression of Myf5 via Gli activator proteins. Myf5 activates expression of miR-133 via upstream E-boxes (Rao et al., 2006; Rosenberg et al., 2006; Sweetman et al., 2008) and we show here that miR-133 directly targets Gli3 via a conserved site in the 3'UTR (Fig. 3E). This site is conserved and was shown to be functional in human Sertoli cells (Yao et al., 2016). We suggest a model whereby Gli3 silencing by miR-133 maintains the finely tuned balance of Gli activator and repressor forms during myogenesis (Fig. 3F). Thus, post-transcriptional silencing of Gli3 in nascent myoblasts promotes the stable activation of the skeletal muscle differentiation programme in response to Gli activators, Gli1 and Gli2 (Fig. 6E). This model is consistent with the finding that concomitant Gli3 knockdown using a morpholino restored myogenic differentiation after miR-133 KD (Fig. 4D). In addition, miR-133 expression, which is initiated by Myf5 in early myoblasts, is mutually exclusive with Gli3 (Fig. S1) (Berti et al., 2015; Mok et al., 2015; Sweetman et al., 2008). In early somites, Gli3 transcripts are

excluded from Myf-5/miR-133 expressing myoblasts and restricted to the dermomyotome, including the dermomyotome lip (Fig. S1C). In differentiating somites, where the myogenic programme is stably established, miR-133 and Gli3 remain expressed in a mutually exclusive fashion, in the myotome or dermomyotome respectively (Goljanek-Whysall et al., 2014; Kahane et al., 2013). In later stage somites, AM133 injection had no effect on myogenin expression (Fig. S2C), suggesting that miR-133 function is essential specifically during early myogenesis. In addition, the lack of a detectable phenotype at later stages shows that there are no non-specific, off-target or toxic effects.

De-repression of Gli3 transcript and protein, following miR-133 KD led to inhibition of the Shh pathway (Fig. 3B, D, F, Fig. 6A), including the down regulation of Gli1 activator, which is important for Myf5 activation (Gustafsson et al., 2002; McDermott et al., 2005). Our results imply direct and indirect consequences resulting from disruption of the Gli1/2 and Gli3 balance in early somites . It is likely that early myoblasts are directly affected, with miR-133 KD leading to loss of stable myogenesis. The finding that concomitant Gli3 KD, using electroporation of a Gli3 MO (Fig. 4D, Fig. S3F), rescued myogenic gene expression suggests that miR-133 mediated post-transciptional regulation of Gli3 is critical to stably establish the myogenic programme. However, myogenic differentiation also involves extracellular matrix production and thus dermomyotome epithelial organization may be affected indirectly.

Shh signal response genes expressed in the myotome include Ptch1 and Ptch2 receptors (Pearse et al., 2001), the Gli1 transcriptional activator, the membrane glycoprotein HHIP (Kahane et al., 2013), which attenuates signalling (Chuang and McMahon, 1999; Ingham and McMahon, 2001), but also Fgf8 (Smith et al., 2005) and the myogenic determination gene, Myf5 (Borycki et al., 1998; McDermott et al., 2005). Differential transcriptomics and RT-qPCR data showed that these genes are negatively affected by miR-133 KD in developing somites (Figs. 3B, D and 6A, B, C). Thus, they are secondary targets of miR-133, but they may be directly regulated by Gli3 repressor (Fig. 3F). Using motif searches we found potential Gli-binding sites within 2kb upstream of transcription start sites in the chicken Ptch1, Ptch2, Myf5 and Fgf8 genes, consistent with Ptch1 and Myf5 being direct targets for Gli proteins (Cohen et al., 2015; Gustafsson et al., 2002).

Other genes down-regulated after miR-133 inhibition such as cell cycle associated genes, CDK1 and CDC20, or sclerotome genes, Pax1 and Pax9 (Fig. 3B), are likely to be indirectly affected through feed-back mechanisms and/or non-cell autonomous mechanisms. For example, the significant downregulation of FGF8 could explain effects on cell proliferation and growth as well as on sclerotome differentiation (Fig. 3B, Fig. 6C). In addition, BMP signals cooperate with Shh to activate somitic chondrogenesis (Murtaugh et al., 1999; Zeng et al., 2002). BMP signalling is likely to be inhibited after miR-133 KD, since Gremlin1 (Grem1), a BMP antagonist, is amongst the top 50 de-repressed genes (Fig. 3B). This provides a possible explanation for negative effects on Pax1 and Pax9 expression. Interestingly, in developing limb buds Gli3 specifies digit identities by promoting cell cycle exit and BMP-dependent chondrogenic differentiation via controlling Grem1 expression (Lopez-Rios et al., 2012).

The role of Gli2 is less clear at present. While we cannot exclude that Gli2 also contributes to the negative regulation of Shh pathway components, we think that this is less likely. Differential transcriptomics showed that Gli2 was slightly de-repressed, however, this was not significant (Fig. 3D) and not confirmed by RT-qPCR (Fig. 5A), and the Gli2 3'UTR has no predicted miR-133 target site. Expression patterns of Gli transcription factors in chick somites are more consistent with the idea that Gli3 is the main repressor of the myogenic programme: Gli1 and Gli2 are expressed in both dermomyotome and myotome, however, Gli3 is excluded from the myotome (Borycki et al., 1998; Kahane et al., 2013).

The effect of miR-133 KD on somite differentiation is dramatic. Expression of myogenic differentiation genes and epithelial organization of the dermomyotome and myotome are severely affected (Figs. 1, 2 and S2A, B). It has been shown that Shh is important for laminin alpha 1 synthesis in the myotome (Anderson et al., 2009), thus suggesting miR-133 KD and the resulting Gli3 de-repression may lead to disrupted BM assembly due to effects on laminin activation. Co-injection with purmporphamine restored BM deposition, indicating that rescue of Gli1, and to some extent Gli2, expression restores the balance of Gli proteins sufficiently to allow laminin synthesis, even in the presence of elevated Gli3 levels (Figs. 4E and 5D).

Shh is also required to maintain the epithelial character of the dermomyotome (Kahane et al., 2013), which was disrupted upon miR-133 KD (Figure 2C) and rescued by purmorphamine co-injection with AM133 (Fig. 5D). Purmorphamine-mediated rescue confirms that stabilisation of the myogenic differentiation programme is intimately linked with cellular organization, and both depend on Shh pathway activity (Fig. 5E). This is in line with the close integration of epithelial morphology and cell fate determination mediated by notch, GSK3β and snail1 during the initiation of myogenesis (Sieiro et al., 2016). On the other hand, myogenesis and epithelialization were uncoupled from proliferation. Proliferation was not rescued due to the continued de-repression of Gli3, which may affect expression of mitotic signals, such as Fgf8, and cell cycle regulators, CDC20 and CDK1 (Fig. 6A, C). Similar observations have previously been made in the limb (Lopez-Rios et al., 2012) and the neural tube (Cayuso et al., 2006; Ulloa et al., 2007). Finally, it has been reported that Shh causes premature myogenic differentiation (Borycki et al., 1999; Kahane et al., 2001; Kahane et al., 2013), which could also explain why proliferation was not rescued.

Together our data uncovers a novel Shh/MRF/miR-133/Gli3 axis whereby miR-133 and its modulation of the Shh signalling pathway via the direct targeting of Gli3 enables the coordination of epithelial morphology with stabilization of the cellular differentiation programme during early myogenesis.

MATERIALS AND METHODS

Somite injections

Fertilised eggs (Henry Stewart, UK) were incubated until the desired stage of development (Hamburger and Hamilton, 1951). Antagomir-133 (AM133) and a scrambled sequence (AMscr), with final concentration of 1 μM, were designed as previously described (Goljanek-Whysall et al., 2011). The posterior six somites of HH14/15 embryos, or the equivalent inter-limb level somites of HH20 embryos, were injected. Embryos were harvested and processed for *in situ* hybridisation or immunohistochemistry, or injected somites were dissected and processed for RNA or protein extraction. Purmorphamine (Sigma) was dissolved in DMSO (2 μM) (Dessaud et al., 2007) and co-

injected with antagomir. Gli3 anti-sense morpholino (MO) was 3' FITC-labelled (Gene-tools) (Supplemental Table S1). Gli3 MO was co-injected with AM133 into the posterior six somites of HH14/15 embryos, followed by electroporation using six 10 msec pulses of 60 V.

In situ hybridisation, immunohistochemistry and image analysis

Whole mount *in situ* hybridisation (WISH) using Digoxigenin-labelled LNA oligo probe for miR-133a (Exiqon) or antisense RNA probes for Pax3, Myf5, MyoD, Mgn, Gli3 (a gift from Matt Towers, University of Sheffield) was carried out as before (Goljanek-Whysall et al., 2011). Antagomirs were detected using anti-FITC antibody coupled to alkaline phosphatase (Roche) as previously described (Goljanek-Whysall et al., 2011). Cryosections (15 µm) of 4% PFA-fixed OCT embedded embryos were immunostained. Primary antibodies: Pax3 (1:200), Pax7 (1:200), Laminin (1:100) from the Developmental Studies Hybridoma Bank (University of Iowa), and anti-rabbit phosphor-histone H3 (1mg/ml, Merck). Phalloidin (Invitrogen) was used at 1:100 to stain actin. Secondary antibodies: anti-rabbit or anti-mouse Alexa Fluor 647 (Invitrogen), 1 mg/ml in 5% BSA/5% goat serum/PBS. DAPI (Sigma) was used at 0.1 mg/ml in PBS. Sections were visualized on an Axioscope with Axiovision software (Zeiss, Germany). Images were imported into Fiji/ImageJ, areas of staining were calculated from binary images by calculating pixel numbers from injected and non-injected sides, when appropriate neural tube staining was removed. A minimum of 10 sections from 3 embryos were analysed for each experiment. Statistical analysis used GraphPad Prism (version 6) software. Mann-Whitney non-parametric two-tail testing was applied to determine P values.

RNA extraction and RT-qPCR

RNA and microRNA isolation from somites used RNAeasy (Qiagen) and miRCURY RNA kits (Exiqon) according to manufacturer's protocols. cDNA was synthesised from 600 ng of RNA using Maxima First Strand cDNA synthesis kit (Thermo Scientific). For microRNAs, cDNA was synthesised from 10 ng using Universal cDNA synthesis kit II (Exiqon). RT-qPCR was performed on a 7500 Fast Real Time PCR machine (Applied Biosystems) using SYBR Green PCR Master Mix (ThermoFisher) according to manufacturer's instructions. Primers for miR-133a sequence

UUGGUCCCCUUCAACCAGCUGU, were designed by Exiqon. Other primers (Sigma) (Supplemental Table S1) were designed with Primer3 software (http://biotools.umassmed.edu/bioapps/primer3_www.cgi). RT-qPCR was normalized to GAPDH for mRNA, or *RNU-6* for miRNA based on Exiqon protocols. Three independent experiments each with three replicate samples were performed for each RT-qPCR. The ΔΔCT (Livak and Schmittgen, 2001) method was used to analyse gene expression levels. Statistical analysis as previously described.

RNA sequencing

Sequencing libraries were built according to Illumina Standard Protocols (Earlham Institute, Norwich, UK), each sample contained pooled, injected somites from 10 embryos. Sequencing was performed on one lane of a flow cell on a Illumina HiSeq2500 platform. cDNA was end-paired, A-tailed and adapter-ligated before amplification and size selection. Library QC used a gel and a bioanalyser. Transcript abundances for each sample were estimated with Kallisto (Bray et al., 2016) using Gallus gallus reference cDNA set (Galgal5) downloaded from Ensembl (Yates et al., 2016). Differential expression (DE) between antagomir-133 (AM133) and scrambled (AMscr) injected samples was calculated using DESeq (Anders and Huber, 2010) with an adjusted p-value significance threshold of 0.05. The data has been uploaded to the NCBI SRA, accession number PRJNA384007. Gene ontology (GO) term analysis was performed using the DAVID Bioinformatics Resources 6.8, available at https://david.ncifcrf.gov/. Statistical analysis was performed using false discovery rate (FDR).

DNA constructs, transfections and luciferase assay

Sensor constructs contained a chick Gli3 3′UTR fragment in a modified pGL3 vector (Promega); for primers see Supplemental Table S1. Mutant construct replaced the miR-133a seed site gggacca with the sequence gttgacaa. Chick dermal fibroblast (DF1) cells were transfected in 96-well plates with 200 ng luciferase reporter plasmid with miR-133 or control (50 nM, Sigma) using Lipofectamine 2000 (Invitrogen). A Renilla luciferase plasmid was included to normalize for transfection efficiency and transfections used triplicate samples. The miRNA mimics were identical to mature miRNA;

sequences in Supplemental Table S1. Firefly and Renilla luciferase activity was measured after 24 hours using a multi-label counter (Promega GloMax) and relative activity was calculated for each sample.

Primary cell culture and western blot

Somites of wild-type embryos were dissected and cultured in DMEM, 10% FBS, 1% pen/strep for 4 hours before being transfected with Gli3 MO (1 mM) or control MO (1 mM) using Endoporter PEG (Gene-tools) and protein extracted after 48 hours. Somites from AM133 or AMscr-injected embryos were dissected for protein extraction. 31.5 µg of protein lysate was run on pre-cast 4-15% polyacrylamide gels (Bio Rad) and blotted onto PVDF membrane (Bio Rad). Primary antibody for Gli3 (1:200, 6F5 Gli3N, Genentech, Wen et al., 2010) was applied 4^{o}C overnight before secondary polyclonal goat anti-mouse HRP (1:1000, P0447, DAKO) was applied for 1 hour at room temperature. The blots were treated with ECL substrate kit (GE Healthcare) and imaged. Primary antibody actin (1:1000, ab3280, Abcam) was applied at 4^{o}C overnight; secondary polyclonal goat anti-mouse HRP was applied for 1 hour at room temperature. The blots were treated with ECL substrate kit and imaged. Quantification of blots was done using ImageJ.

Acknowledgements

We thank all members of the Münsterberg and Wheeler labs for discussions, James Briscoe and Matt Towers for sharing plasmids and Paul Thomas for assistance with microscopy. This work was funded by grants from the Biotechnology and Biological Sciences Research Council (BBSRC) reference BB/K003437 and BB/N007034 to AM

Competing interests

This is to confirm that the authors have no financial or non-financial competing interests.

References

Abou-Elhamd, A., Alrefaei, A.F., Mok, G.F., Garcia-Morales, C., Abu-Elmagd, M., Wheeler, G.N. and Munsterberg, A.E. (2015). Klhl31 attenuates beta-catenin dependent Wnt signaling and regulates embryo myogenesis. *Dev Biol* **402**, 61-71.

Abu-Elmagd, M., Robson, L., Sweetman, D., Hadley, J., Francis-West, P. and Munsterberg, A. (2010). Wnt/Lef1 signaling acts via Pitx2 to regulate somite myogenesis. *Dev Biol* **337**, 211-219.

Ahmed, A., Ward, N.J., Moxon, S., Lopez-Gomollon, S., Viaut, C., Tomlinson, M.L., Patrushev, I., Gilchrist, M.J., Dalmay, T., Dotlic, D. *et al.* (2015). A Database of microRNA Expression Patterns in Xenopus laevis. *PLoS One* **10**, e0138313.

Alteri, A., De Vito, F., Messina, G., Pompili, M., Calconi, A., Visca, P., Mottolese, M., Presutti, C. and Grossi, M. (2013). Cyclin D1 is a major target of miR-206 in cell differentiation and transformation. *Cell Cycle* **12**, 3781-3790.

Anders, S. and Huber, W. (2010). Differential expression analysis for sequence count data. *Genome Biol* **11**, R106.

Anderson, C., Thorsteinsdottir, S. and Borycki, A.G. (2009). Sonic hedgehog-dependent synthesis of laminin alpha1 controls basement membrane assembly in the myotome. *Development* **136**, 3495-3504.

Bartel, D.P. (2009). MicroRNAs: target recognition and regulatory functions. *Cell* **136**, 215-233.

Berti, F., Nogueira, J.M., Wohrle, S., Sobreira, D.R., Hawrot, K. and Dietrich, S. (2015). Time course and side-by-side analysis of mesodermal, pre-myogenic, myogenic and differentiated cell markers in the chicken model for skeletal muscle formation. *J Anat* **227**, 361-382.

Bethune, J., Artus-Revel, C.G. and Filipowicz, W. (2012). Kinetic analysis reveals successive steps leading to miRNA-mediated silencing in mammalian cells. *EMBO Rep* **13**, 716-723.

Boettger, T., Wust, S., Nolte, H. and Braun, T. (2014). The miR-206/133b cluster is dispensable for development, survival and regeneration of skeletal muscle. *Skelet Muscle* **4**, 23.

Borycki, A.G., Brunk, B., Tajbakhsh, S., Buckingham, M., Chiang, C. and Emerson, C.P., Jr. (1999). Sonic hedgehog controls epaxial muscle determination through Myf5 activation. *Development* **126**, 4053-4063.

Borycki, A.G., Mendham, L. and Emerson, C.P., Jr. (1998). Control of somite patterning by Sonic hedgehog and its downstream signal response genes. *Development* **125**, 777-790.

Bray, N.L., Pimentel, H., Melsted, P. and Pachter, L. (2016). Near-optimal probabilistic RNA-seq quantification. *Nat Biotechnol* **34**, 525-527.

Buckingham, M. and Rigby, P.W. (2014). Gene regulatory networks and transcriptional mechanisms that control myogenesis. *Dev Cell* **28**, 225-238.

Cayuso, J., Ulloa, F., Cox, B., Briscoe, J. and Marti, E. (2006). The Sonic hedgehog pathway independently controls the patterning, proliferation and survival of neuroepithelial cells by regulating Gli activity. *Development* **133**, 517-528.

Chen, J.F., Mandel, E.M., Thomson, J.M., Wu, Q., Callis, T.E., Hammond, S.M., Conlon, F.L. and Wang, D.Z. (2006). The role of microRNA-1 and microRNA-133 in skeletal muscle proliferation and differentiation. *Nat Genet* **38**, 228-233.

Christ, B. and Scaal, M. (2008). Formation and differentiation of avian somite derivatives. *Adv Exp Med Biol* **638**, 1-41.

Chuang, P.T. and McMahon, A.P. (1999). Vertebrate Hedgehog signalling modulated by induction of a Hedgehog-binding protein. *Nature* **397**, 617-621.

Cohen, M., Kicheva, A., Ribeiro, A., Blassberg, R., Page, K.M., Barnes, C.P. and Briscoe, J. (2015). Ptch1 and Gli regulate Shh signalling dynamics via multiple mechanisms. *Nat Commun* **6**, 6709.

Darnell, D.K., Kaur, S., Stanislaw, S., Konieczka, J.H., Yatskievych, T.A. and Antin, P.B. (2006). MicroRNA expression during chick embryo development. *Dev Dyn* **235**, 3156-3165.

Dessaud, E., Yang, L.L., Hill, K., Cox, B., Ulloa, F., Ribeiro, A., Mynett, A., Novitch, B.G. and Briscoe, J. (2007). Interpretation of the sonic hedgehog morphogen gradient by a temporal adaptation mechanism. *Nature* **450**, 717-720.

Ebert, M.S. and Sharp, P.A. (2012). Roles for microRNAs in conferring robustness to biological processes. *Cell* **149**, 515-524.

Feng, Y., Niu, L.L., Wei, W., Zhang, W.Y., Li, X.Y., Cao, J.H. and Zhao, S.H. (2013). A feedback circuit between miR-133 and the ERK1/2 pathway involving an exquisite mechanism for regulating myoblast proliferation and differentiation. *Cell Death Dis* **4**, e934.

Goljanek-Whysall, K., Mok, G.F., Fahad Alrefaei, A., Kennerley, N., Wheeler, G.N. and Munsterberg, A. (2014). myomiR-dependent switching of BAF60 variant incorporation into Brg1 chromatin remodeling complexes during embryo myogenesis. *Development* **141**, 3378-3387.

Goljanek-Whysall, K., Pais, H., Rathjen, T., Sweetman, D., Dalmay, T. and Münsterberg, A. (2012). Regulation of multiple target genes by miR-1 and miR-206 is pivotal for C2C12 myoblast differentiation. *J Cell Sci* **125**, 3590-3600.

Goljanek-Whysall, K., Sweetman, D., Abu-Elmagd, M., Chapnik, E., Dalmay, T., Hornstein, E. and Münsterberg, A. (2011). MicroRNA regulation of the paired-box transcription factor Pax3 confers robustness to developmental timing of myogenesis. *Proc Natl Acad Sci U S A* **108**, 11936-11941.

Gros, J., Scaal, M. and Marcelle, C. (2004). A two-step mechanism for myotome formation in chick. *Dev Cell* **6**, 875-882.

Gustafsson, M.K., Pan, H., Pinney, D.F., Liu, Y., Lewandowski, A., Epstein, D.J. and Emerson, C.P., Jr. (2002). Myf5 is a direct target of long-range Shh signaling and Gli regulation for muscle specification. *Genes Dev* **16**, 114-126.

Hamburger, V. and Hamilton, H.L. (1951). A series of normal stages in the development of the chick embryo. *J Morphol* **88**, 49-92.

Horak, M., Novak, J. and Bienertova-Vasku, J. (2016). Muscle-specific microRNAs in skeletal muscle development. *Dev Biol* **410**, 1-13.

Hornstein, E. and Shomron, N. (2006). Canalization of development by microRNAs. *Nat Genet* **38**, S20-24.

Ingham, P.W. and McMahon, A.P. (2001). Hedgehog signaling in animal development: paradigms and principles. *Genes Dev* **15**, 3059-3087.

Johnson, R.L., Laufer, E., Riddle, R.D. and Tabin, C. (1994). Ectopic expression of Sonic hedgehog alters dorsal-ventral patterning of somites. *Cell* **79**, 1165-1173.

Kahane, N., Cinnamon, Y., Bachelet, I. and Kalcheim, C. (2001). The third wave of myotome colonization by mitotically competent progenitors: regulating the balance between differentiation and proliferation during muscle development. *Development* **128**, 2187-2198.

Kahane, N., Ribes, V., Kicheva, A., Briscoe, J. and Kalcheim, C. (2013). The transition from differentiation to growth during dermomyotome-derived myogenesis depends on temporally restricted hedgehog signaling. *Development* **140**, 1740-1750.

Liu, N., Bezprozvannaya, S., Shelton, J.M., Frisard, M.I., Hulver, M.W., McMillan, R.P., Wu, Y., Voelker, K.A., Grange, R.W., Richardson, J.A. *et al.* (2011). Mice lacking microRNA 133a develop dynamin 2-dependent centronuclear myopathy. *J Clin Invest* **121**, 3258-3268.

Liu, N., Williams, A.H., Kim, Y., McAnally, J., Bezprozvannaya, S., Sutherland, L.B., Richardson, J.A., Bassel-Duby, R. and Olson, E.N. (2007). An intragenic MEF2-dependent enhancer directs muscle-specific expression of microRNAs 1 and 133. *Proc Natl Acad Sci U S A* **104**, 20844-20849.

Livak, K.J. and Schmittgen, T.D. (2001). Analysis of relative gene expression data using real-time quantitative PCR and the 2-ΔΔCT method. *Methods* **25**, 402-408.

Lopez-Rios, J., Speziale, D., Robay, D., Scotti, M., Osterwalder, M., Nusspaumer, G., Galli, A., Hollander, G.A., Kmita, M. and Zeller, R. (2012). GLI3 constrains digit number by controlling both progenitor proliferation and BMP-dependent exit to chondrogenesis. *Dev Cell* **22**, 837-848.

McDermott, A., Gustafsson, M., Elsam, T., Hui, C.C., Emerson, C.P., Jr. and Borycki, A.G. (2005). Gli2 and Gli3 have redundant and context-dependent function in skeletal muscle formation. *Development* **132**, 345-357.

Mishima, Y., Abreu-Goodger, C., Staton, A.A., Stahlhut, C., Shou, C., Cheng, C., Gerstein, M., Enright, A.J., and Giraldez, A.J. (2009). Zebrafish miR-1 and miR-133 shape muscle gene expression and regulate sarcomeric actin organization. *Genes Dev* **23**, 619-632.

Mok, G.F., Lozano-Velasco, E. and Münsterberg, A. (2017). microRNAs in skeletal muscle development. *Seminars in Cell and Developmental Biology* **72**, 67-76.

Mok, G.F., Mohammed, R.H. and Sweetman, D. (2015). Expression of myogenic regulatory factors in chicken embryos during somite and limb development. *J Anat* **227**, 352-360.

Mok, G.F. and Sweetman, D. (2011). Many routes to the same destination: lessons from skeletal muscle development. *Reproduction* **141**, 301-312.

Münsterberg, A.E., Kitajewski, J., Bumcrot, D.A., McMahon, A.P. and Lassar, A.B. (1995). Combinatorial signaling by Sonic hedgehog and Wnt family members induces myogenic bHLH gene expression in the somite. *Genes Dev* **9**, 2911-2922.

Murtaugh, L.C., Chyung, J.H. and Lassar, A.B. (1999). Sonic hedgehog promotes somitic chondrogenesis by altering the cellular response to BMP signaling. *Genes Dev* **13**, 225-237.

Pearse, R.V., 2nd, Vogan, K.J. and Tabin, C.J. (2001). Ptc1 and Ptc2 transcripts provide distinct readouts of Hedgehog signaling activity during chick embryogenesis. *Dev Biol* **239**, 15-29.

Rao, P.K., Kumar, R.M., Farkhondeh, M., Baskerville, S. and Lodish, H.F. (2006). Myogenic factors that regulate expression of muscle-specific microRNAs. *Proc Natl Acad Sci U S A* **103**, 8721-8726.

Rios, A.C., Serralbo, O., Salgado, D. and Marcelle, C. (2011). Neural crest regulates myogenesis through the transient activation of NOTCH. *Nature* **473**, 532-535.

Rosenberg, M.I., Georges, S.A., Asawachaicharn, A., Analau, E. and Tapscott, S.J. (2006). MyoD inhibits Fstl1 and Utrn expression by inducing transcription of miR-206. *J Cell Biol* **175**, 77-85.

Sieiro, D., Rios, A.C., Hirst, C.E. and Marcelle, C. (2016). Cytoplasmic NOTCH and membrane-derived beta-catenin link cell fate choice to epithelial-mesenchymal transition during myogenesis. *Elife 5*.

Sinha, S. and Chen, J.K. (2006). Purmorphamine activates the Hedgehog pathway by targeting Smoothened. *Nat Chem Biol **2***, 29-30.

Smith, T.G., Sweetman, D., Patterson, M., Keyse, S.M. and Münsterberg, A. (2005). Feedback interactions between MKP3 and ERK MAP kinase control scleraxis expression and the specification of rib progenitors in the developing chick somite. *Development* **132**, 1305-1314.

Sweetman, D., Goljanek, K., Rathjen, T., Oustanina, S., Braun, T., Dalmay, T. and Münsterberg, A. (2008). Specific requirements of MRFs for the expression of muscle specific microRNAs, miR-1, miR-206 and miR-133. *Dev Biol* **321**, 491-499.

Teboul, L., Hadchouel, J., Daubas, P., Summerbell, D., Buckingham, M. and Rigby, P.W. (2002). The early epaxial enhancer is essential for the initial expression of the skeletal muscle determination gene Myf5 but not for subsequent, multiple phases of somitic myogenesis. *Development* **129**, 4571-4580.

Trajkovski, M., Ahmed, K., Esau, C.C. and Stoffel, M. (2012). MyomiR-133 regulates brown fat differentiation through Prdm16. *Nat Cell Biol* **14**, 1330-1335.

Ulloa, F., Itasaki, N. and Briscoe, J. (2007). Inhibitory Gli3 activity negatively regulates Wnt/beta-catenin signaling. *Curr Biol* **17**, 545-550.

Wen, X., Lai, C. K., Evangelista, M., Hongo, J. A., de Sauvage, F. J. and Scales, S. J. (2010). Kinetics of hedgehog-dependent full-length Gli3 accumulation in primary cilia and subsequent degradation. *Mol Cell Biol* **30**, 1910-1922.

Wystub, K., Besser, J., Bachmann, A., Boettger, T. and Braun, T. (2013). miR-1/133a clusters cooperatively specify the cardiomyogenic lineage by adjustment of myocardin levels during embryonic heart development. *PLoS Genet* **9**, e1003793.

Yao, C., Sun, M., Yuan, Q., Niu, M., Chen, Z., Hou, J., Wang, H., Wen, L., Liu, Y., Li, Z. and He, Z (2016). MiRNA-133b promotes the proliferation of human Sertoli cells through targeting GLI3. *Oncotarget* **7**, 2201-2219.

Yates, A., Akanni, W., Amode, M.R., Barrell, D., Billis, K., Carvalho-Silva, D., Cummins, C., Clapham, P., Fitzgerald, S., Gil, L. *et al.* (2016). Ensembl 2016. *Nucleic Acids Res* **44**, D710-716.

Zeng, L., Kempf, H., Murtaugh, L.C., Sato, M.E. and Lassar, A.B. (2002). Shh establishes an Nkx3.2/Sox9 autoregulatory loop that is maintained by BMP signals to induce somitic chondrogenesis. *Genes Dev* **16**, 1990-2005.

Figures

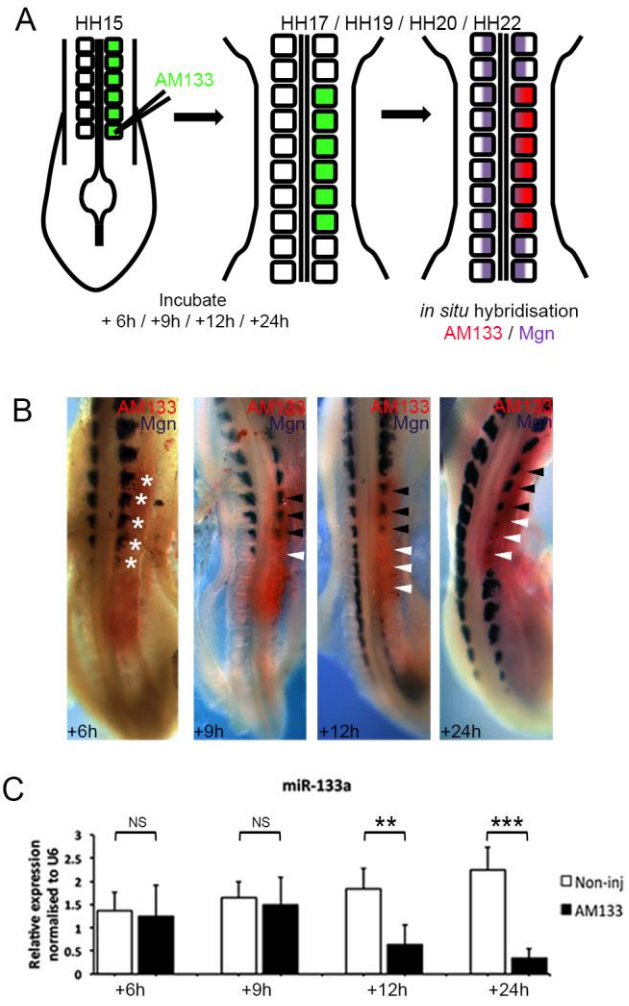

Fig. 1. Inhibition of miR-133 leads to a myogenic phenotype. (A) Schematic overview of the experimental approach. Posterior somites of HH14/15 embryos were injected with FITC-labelled antagomiR-133 (AM133) and the downstream analysis performed by *in situ* hybridization. (B) Embryos incubated for 6, 9, 12 and 24 hours after antagomir-133 (AM133) injection as indicated. *In situ* hybridization detects transcripts for myogenin (Mgn, purple) and FITC- antagomir is detected in red. After 6 hours there is no change in myogenin expression in injected somites (white asterisks, n=7/8). After 9 hours the most posterior somites show a loss (white arrowheads) or reduced (black arrowheads) myogenin expression (n=12/16). The negative effect on myogenic differentiation becomes more pronounced after 12 hours and 24 hours (n=8/8, n=14/14). (C) RT-qPCR for miR-133

of somites, pooled from a minimum of 4 embryos, injected with AM133 compared to contralateral non-injected somites, harvested after 6, 9, 12 or 24 hours of incubation as indicated. ***p value < 0.001; **p value 0.001 to 0.01; ns, not significant.

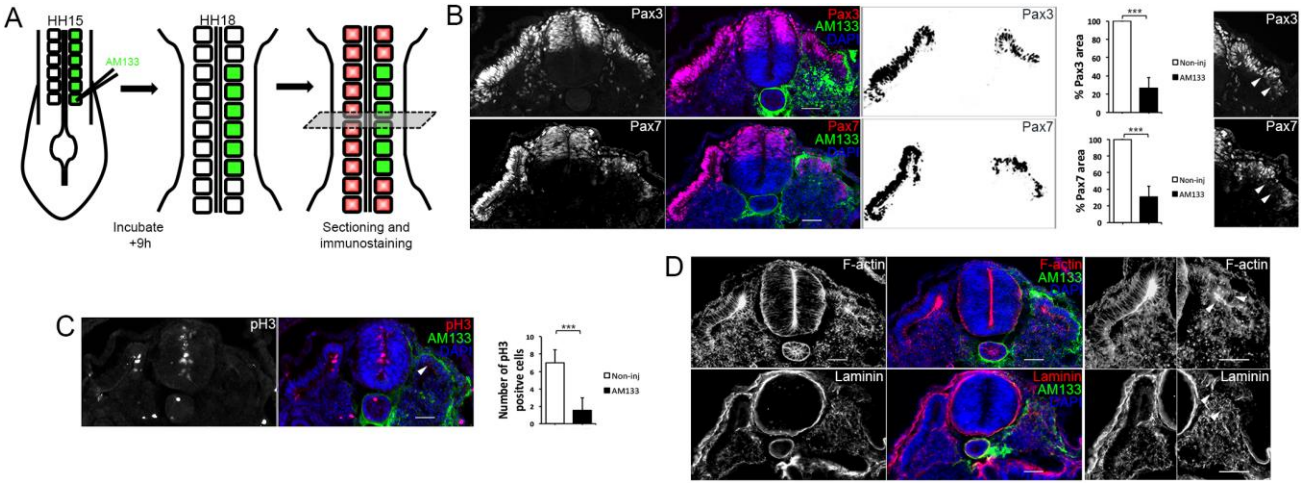

Fig. 2. Dermomyotome growth, epithelial organization and basement membrane deposition are disrupted after inhibition of miR-133. (A) Schematic overview of the experimental approach. Posterior somites of HH14/15 embryos were injected with FITC-labelled antagomiR-133 (AM133) and the downstream analysis performed by immunostaining after 9 hours incubation. (B) Immunostaining for Pax3, Pax7, FITC and DAPI as indicated. The areas positive for Pax3 or Pax7 staining within the somite were quantified using Fiji/ImageJ and were significantly smaller in AM133 injected somites compared to non-injected contralateral control side. Higher magnification images of injected somites showed disruption to dermomyotome morphology (white arrowheads). (C) Immunostaining for pH3, FITC and DAPI as indicated. The number of pH3-positive cells was significantly reduced in AM133 injected somites (white arrowheads) compared to the contralateral side. ***p value < 0.001. (D) Immunostaining for F-actin, laminin, FITC and DAPI as indicated. Higher magnification images of non-injected and injected somites stained for F-actin or laminin. White arrowheads indicate disorganized and disrupted staining in the dermomyotome region. Scale bar 50 μm.

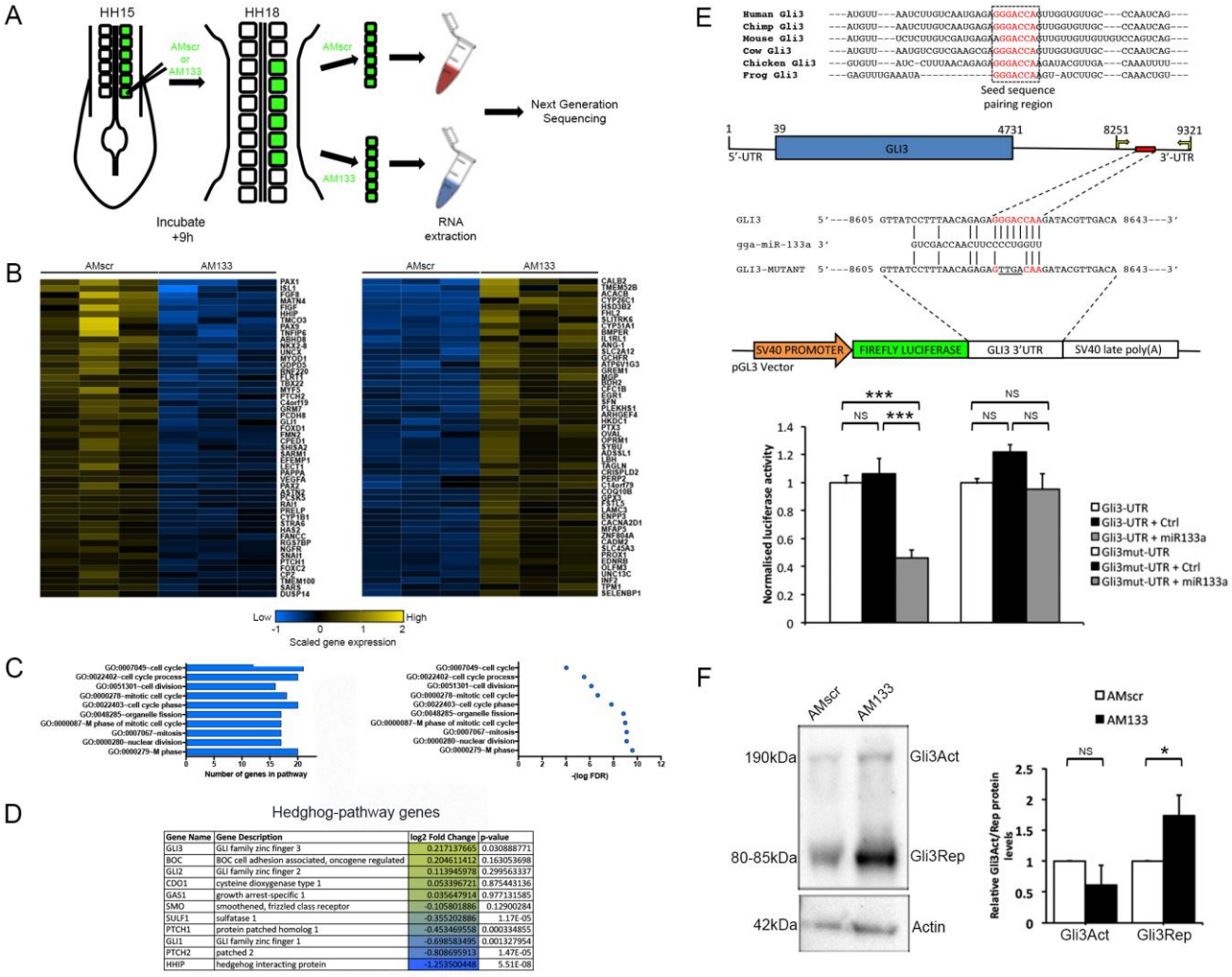

Gene Name	Gene Description	log2 Fold Change	p-value
GLI3	GLI family zinc finger 3	0.217137665	0.030888771
BOC	BOC cell adhesion associated, oncogene regulated	0.204611412	0.163053698
GLI2	GLI family zinc finger 2	0.113945978	0.299563337
CDO1	cysteine dioxygenase type 1	0.053396721	0.875443136
GAS1	growth arrest-specific 1	0.035647914	0.977131585
SMO	smoothened, frizzled class receptor	-0.105801886	0.12900284
SULF1	sulfatase 1	-0.355202886	1.17E-05
PTCH1	protein patched homolog 1	-0.453469558	0.000334855
GLI1	GLI family zinc finger 1	-0.698583495	0.001327954
PTCH2	patched 2	-0.808695913	1.47E-05
HHIP	hedgehog interacting protein	-1.253500448	5.51E-08

Fig. 3. Differential transcriptomics reveals mis-regulation of Shh pathway components and identifies Gli3 as direct miR-133 target. (A) Schematic overview of the experimental approach. Posterior somites of HH14/15 embryos were injected with FITC-labelled antagomiR-133 (AM133) or scrambled-antagomir (AMscr) and harvested after 9 hours for RNA isolation and sequencing. (B) Heatmaps of the top 50 genes significantly downregulated or upregulated after miR-133 knock-down shows clustering of six samples injected with AMscr or with AM133. (C) Gene ontology (GO) analysis showed that amongst the downregulated differentially expressed (DE) group, genes associated with cell cycle processes were significantly overrepresented. The false discovery rates (FDRs) are shown for these genes. (D) Table showing Hedgehog (Hh) pathway genes that were de-repressed (yellow) and repressed (blue) including the transcriptional regulator Gli3, with log2 fold change and p-values. (E) Conservation of miR-133 seed sequence pairing region within the Gli3 3'UTR of different species.

Luciferase assays validate Gli3 as a direct target for miR-133. Schematic of the chick Gli3 gene with a predicted target site containing an 8-mer seed match (red) present in the 3'UTR. Mutations (underlined) introduced into the predicted target site were designed to disrupt base pairing with the miR-133 seed region. A modified pGL3 vector containing a 1070 bp fragment of the chick Gli3 3'UTR downstream of the firefly luciferase reporter gene. Transfection of reporter plasmids into DF1 cells either on its own (white), or with a control miR mimic (black), or with miR-133 mimic (grey) confirms negative regulation of the reporter. The response was rescued after mutation of the target site. ***p value < 0.001; ns, not significant. (F) Western blot of somites injected with AMscr or AM133 shows increased amount of Gli3Rep protein. Quantitative analysis was performed on three biological replicates. *p value < 0.1, ns, not significant.

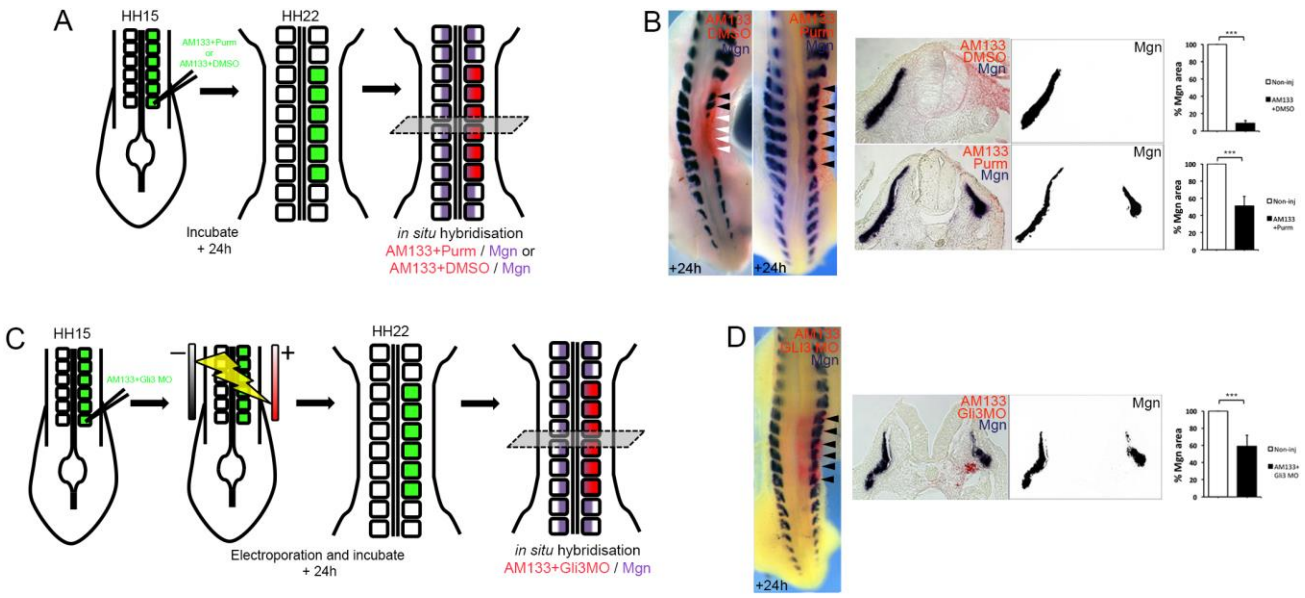

Fig. 4. Pharmacological activation of Shh pathway or Gli3 knock down restores myogenesis in absence of miR-133 function. (A) Schematic overview of the experimental approach. Posterior somites of HH14/15 embryos were injected with FITC-labelled antagomiR-133 (AM133) with purmorphamine (purm) or FITC-labelled scrambled-antagomir (AMscr) with DMSO as control and the downstream analysis performed by *in situ* hybridization after 24 hours incubation. (B) *In situ* hybridization showed that myogenin (Mgn) expression was lost (white arrowheads) after AM133 with DMSO injection, n=8/8. Co-injection of AM133 with purmorphamine, a synthetic agonist of the smoothened receptor, rescued myogenesis (black arrowheads). Mgn was expressed and the epithelial nature of the dermomyotome was preserved, but myotome size was reduced, n=14/14. Whole mount and sections are shown. (C) Schematic overview of the experimental approach. Posterior somites of HH14/15 embryos were injected with FITC-labelled antagomiR-133 (AM133) with Gli3 morpholino (MO), electroporated and the downstream analysis performed by *in situ* hybridization after 24 hours incubation. (D) Co-transfection of AM133 with Gli3 MO rescued myogenesis (black arrowheads), although myotome size was reduced (n=7/10). Whole mount and sections are shown. Area measurements obtained using Fiji/ImageJ. ***p value < 0.001.

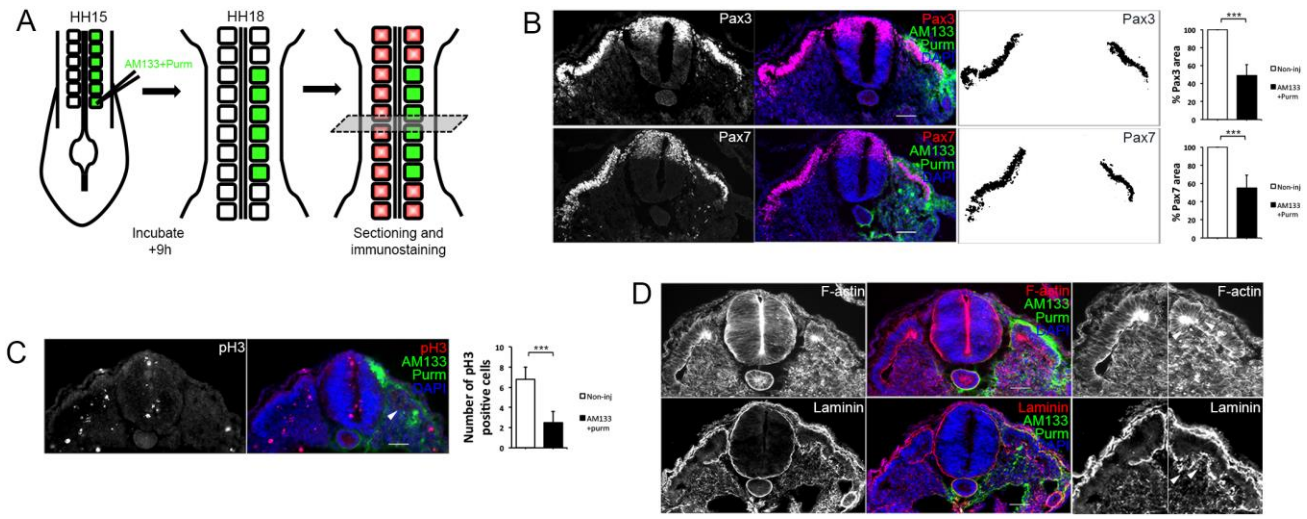

Fig. 5. Shh pathway activation in antagomir-133 injected somites restores dermomyotome morphology, epithelial organisation and basement membrane desposition but not proliferation. (A) Schematic overview of the experimental approach. Posterior somites of HH14/15 embryos were injected with FITC-labelled antagomiR-133 (AM133) with purmorphamine (purm) and the downstream analysis performed by immunostaining after 9 hours incubation. (B) Immunostaining for Pax3 or Pax7, FITC and DAPI, and area measurements after AM133 with purmorphamine injections. (C) Immunostaining for pH3, FITC and DAPI, and counting of positive cells after AM133 plus purmorphamine injections. The number of pH3-positive cells was reduced (white arrowheads) in AM133 with purmorphamine injected somites compared to the contralateral side. (D) Epithelial organization and basement membrane deposition were improved after co-injection of purmorphamine with AM133. Immunostaining for F-actin, laminin, FITC and DAPI as indicated. Higher magnification of non-injected and injected somites with the dermomyotome, dorsomedial lip, and more continuous BM staining beneath the myotome indicated by white arrowheads. Scale bar 50 μm. ***p value < 0.001.

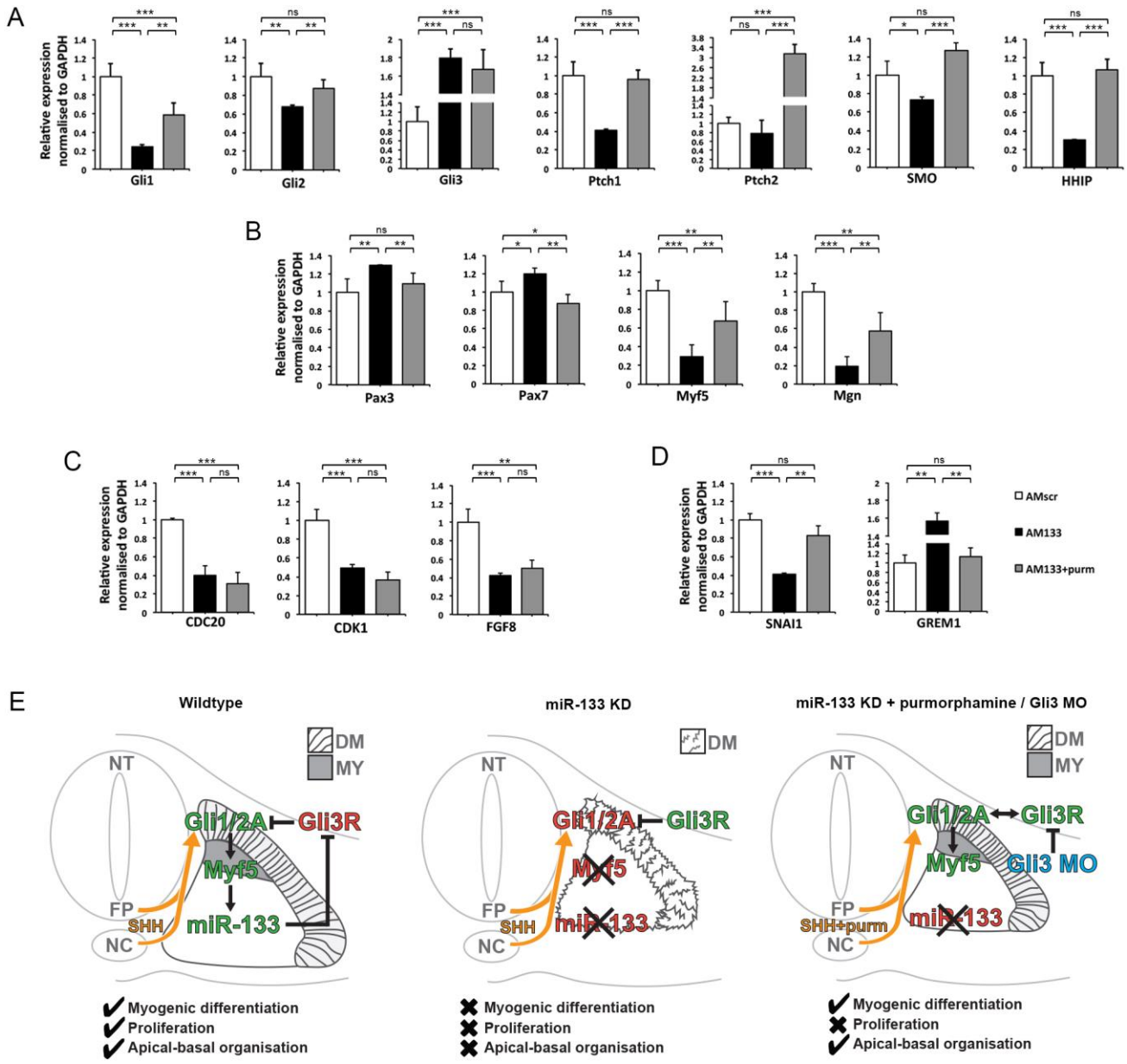

Fig. 6. Purmorphamine restores expression of Shh pathway and myogenic genes, however, Gli3 and cell cycle genes remain de-regulated in absence of miR-133 function. (A) RT-qPCR for Shh pathway components, (B) myogenic genes, (C) cell cycle genes and (D) a regulator of EMT and BMP signalling, as indicated. White columns represent somites injected with scrambled antagomir (AMscr), black columns represent somites injected with antagormiR-133 (AM133), grey columns represent somites injected with AM133 with purmorphamine. (E) Summary of regulatory interactions identified in this study, see text for details. NT, neural tube; FP, floor plate; NC, notochord; DM,

Supplemental figures

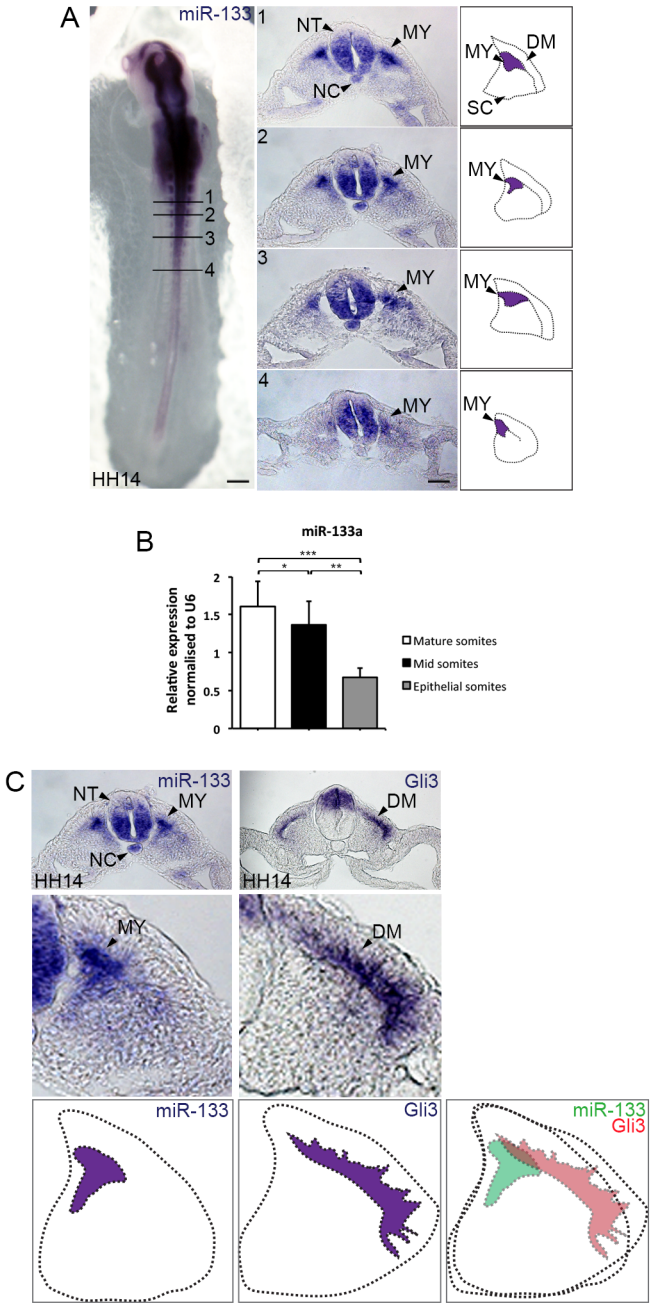

Fig. S1. Expression of miR-133 in developing somites. Whole mount *in situ* hybridization using double Digoxigenin-labelled LNA probes (Exiqon) shows restricted expression of miR-133 in the neural tube (NT), anterior notochord (NC) and medial somites but no expression in the sclerotome (SC). (A) HH14 stage embryo, 1-4 indicates levels of cryosections shown in panels 1-4, with a schematic representing somite expression. (B) RT-qPCR for miR-133 shows a relative increase of expression in more mature, anterior somites compared to posterior epithelial somites, 8 biological replicates. ***p value < 0.001; **p value 0.001 to 0.01; *p value 0.01 to 0.1. Scale bar, 200 μm in panel A; 50 μm in panel 4. (C) Comparison of miR-133 and Gli3 expression in developing somites. Higher magnification of somites show miR-133 expressed in nascent myoblasts (MY) and Gli3 in the dermomyotome (DM).

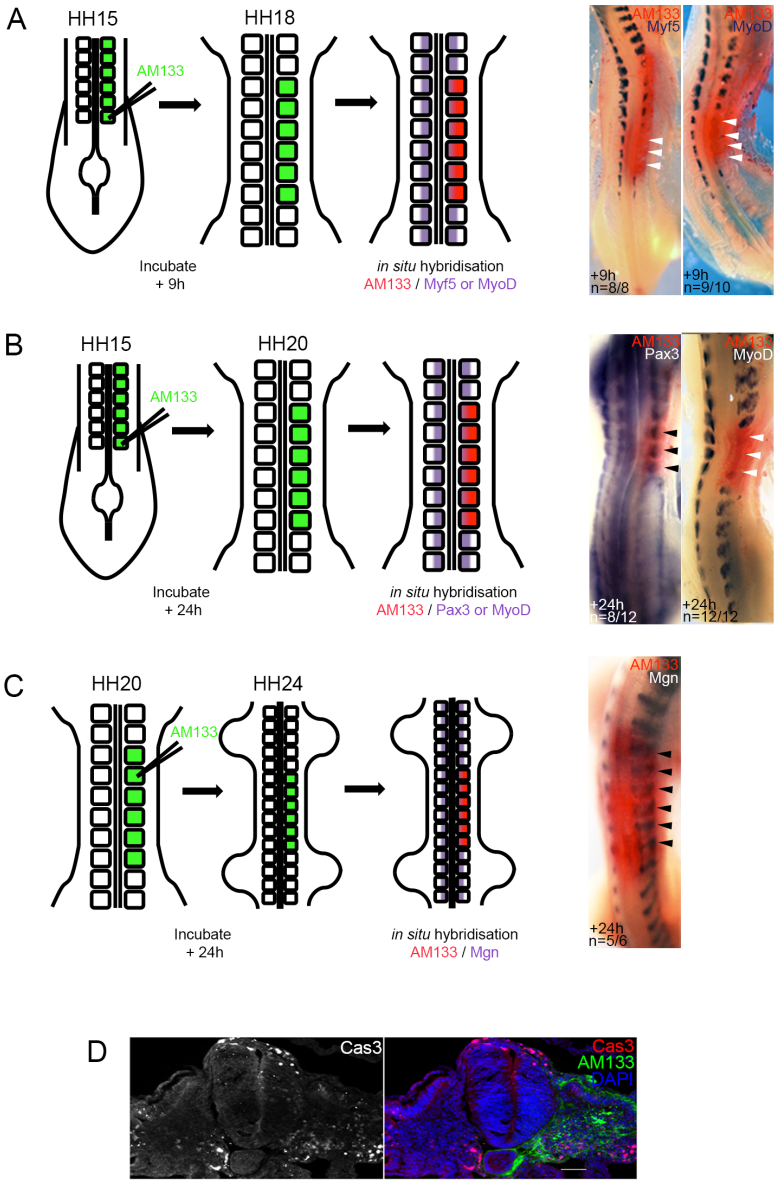

Fig. S2. Inhibition of miR-133 leads to a myogenic phenotype in early somites, but not in differentiating somites. Embryos were injected with FITC-labelled antagomir-133 (AM133) at HH14/15 or HH20. Whole mount *in situ* hybridisation was performed for Myf5, MyoD, Mgn or Pax3 as indicated. (A) 9 hour incubation, (B) 24 hour incubation post-injection. (C) AM133-injected into inter-limb somites at HH20 and incubated for 24 hours. Antisense probes (purple), FITC-labelled antagomir (red). Number of embryos indicated on each panel. White arrowheads indicating loss of expression on injected side; black arrowheads indicating reduced expression or no change in expression on injected side. (D) Immunostaining for Cas3, an apoptosis marker, in embryos injected with AM133 at HH14/15 and incubated for 9 hours show no difference in AM133 injected side compared to contralateral non-injected side. Scale bar 50 μm.

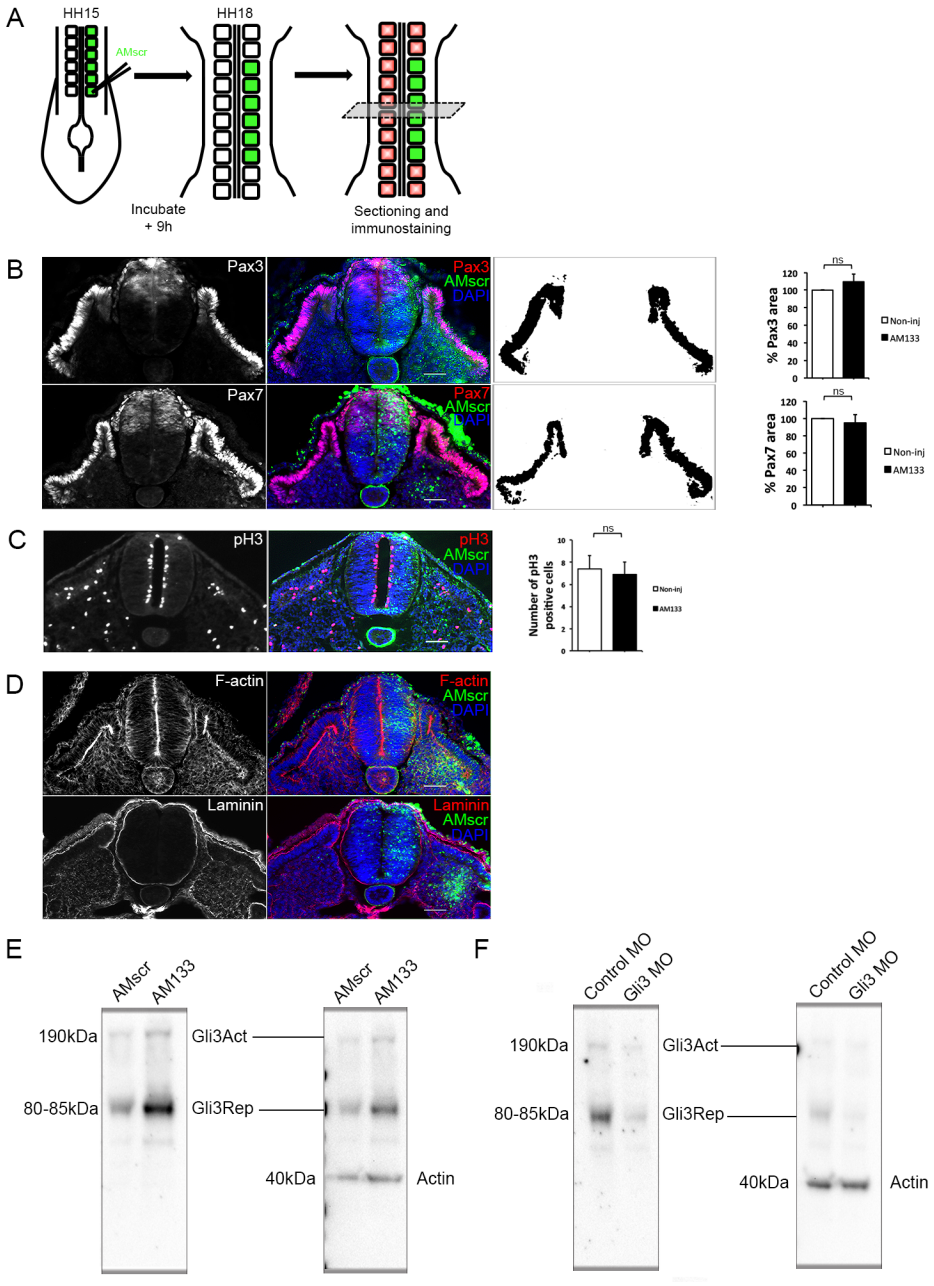

Fig. S3. Dermomyotome growth, epithelial organization and basement membrane deposition are not affected by injection of a scrambled antagomir. (A) Schematic representation of the experimental procedure. Somites of HH14/15 embryos were injected with FITC-labelled scrambled antagomir (AMscr) and processed for immunostaining after 9 hours. (B) Somites were cryosectioned and immunostained for Pax3, Pax7, FITC and DAPI as indicated. The areas positive for Pax3 or Pax7 staining within the somite were quantified using Fiji/ImageJ. There was no significant difference between injected and non-injected contralateral control side. (C) Immunostaining for pH3, FITC and DAPI as indicated. The number of pH3-positive cells was similar in AMscr injected somites compared to the contralateral side. Scale bar 50 µm; ns, not significant. (D) Immunostaining for F-actin, laminin, FITC and DAPI as indicated. Epithelial organization and basement membrane deposition were not affected and were similar on both sides. Scale bar 50 µm; ns, not significant. (E) Western blot detecting Gli3 protein in somites injected with AMscr or AM133 shows increased level of Gli3Rep

protein after miR-133 KD. (F) Western blot detecting Gli3 protein in primary cultured somites transfected with control MO or Gli3 MO shows reduced Gli3 protein after Gli3 MO.

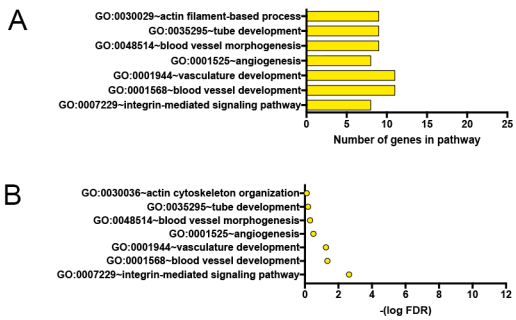

Fig. S4: Differential transcriptomics of somites after miR-133 KD. (A) Gene Ontology (GO) terms of genes expressed at higher levels in AM133 injected somites were associated with angiogenesis and tube morphogenesis. (B) However, the false discovery rates (FDRs) for these were significantly higher compared to GO terms associated with the downregulated DE genes.

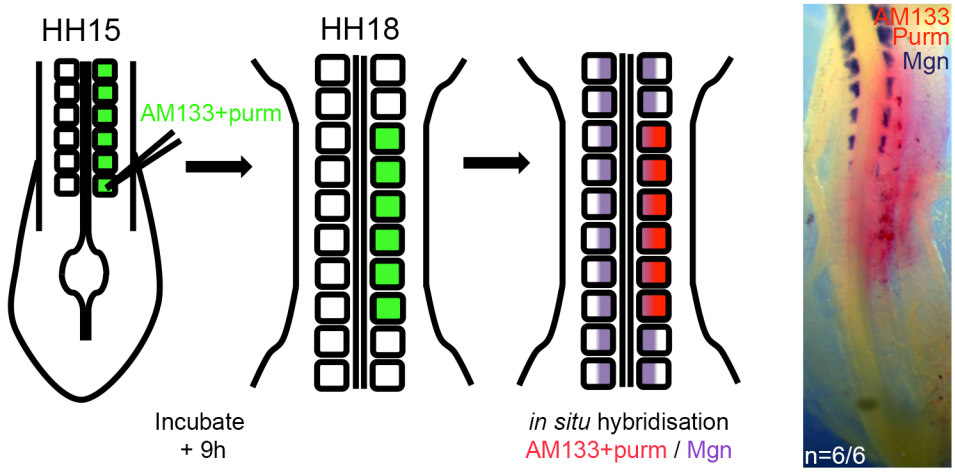

Fig. S5. Purmorphamine mediated activation of the Shh pathway rescues myogenic differentiation in absence of miR-133 function. Co-injection of FITC-labelled antagomir-133 (AM133) and purmorphamine (purm) into HH14/15 embryos was examined by *in situ* hybridisation for myogenin (Mgn) transcripts, which indicates normal expression after 9 hours incubation (n=6/6). Mgn antisense probe (purple), FITC-labelled antagomir (red).

Table S1 – PCR and mutagenesis primers, mimics and siRNA

cGli1 RT F	ACCTCTCCATCAGCACCATC
cGli1 RT R	TTGGCTGTCAGAGGGCTACT
cGli2 RT F	CACCATCAGCTCTGCCTACA
cGli2 RT R	TGAGCTGGTGTGAGGTTCAG
cGli3 RT F	CTCACCTCTTTCCAGCGTTC
cGli3 RT R	AATGTACGGGTGAGGAGTGC
cPtch1 RT F	GTGGAAGTTGGTGGACGAGT
cPtch1 RT R	CATGTACTCTGCTGGCCTGA
cPtch2 RT F	GAGTGAGGAGAAGGCAGGTG
cPtch2 RT R	CATGGTGACACAGGCATAGG
cSmo RT F	GACAACCCCAAGAGCTGGTA
cSmo RT R	CACAAAGAAGCAGGCATTGA
cHHIP RT F	CCCTCGACGATATGGAAGAA
cHHIP RT R	GTGGTGATCCACAGCACATC
cPax3 RT F	AGCAGAGCAACTGGAAGAGC
cPax3 RT R	GGTGGTTGAAAGCCATCAGT
cPax7 RT F	GCATCAAATTCGGGAAGAAA
cPax7 RT R	CTCTTCAAAGGCAGGTCTGG
cMyf5 RT F	CAACCCCAACCAGAGACTCC
cMyf5 RT R	GAGTCCGCCATCACATCGGA
cMgn RT F	GGCTTTGGAGGAGAAGGACT
cMgn RT R	CAGAGTGCTGCGTTTCAGAG
cCDC20 RT F	CCCTCAGCTGGAACAGCTAC
cCDC20 RT R	TGGTGCTGAGTGAAGGTCTG
cCDK1 RT F	TATAAAGGGCGCCACAAAAC
cCDK1 RT R	TCTTGAGGTCCATGGAAAGG
cFGF8 RT F	AGCAGAGCCTGGTGACAGAT
cFGF8 RT R	TTTCCCCTTCTTGTTCATGC
cSNAI1 RT F	CGATGCTCAGACCAGGAAAT
cSNAI1 RT R	AAGGGCTTTTCACCAGTGTG
cGREM1 RT F	AGGCACTGCACATCACTGAG
cGREM1 RT R	TCAGGGCAGTTGAGGGTAAC
cGAPDH RT F	TCTCTGGCAAAGTCCAAGTG
cGAPDH RT R	TCACAAGTTTCCCGTTCTCAG
cGLI3-UTR F	GCAGATCT TTTCACTTTCCACAAATCTGG
cGLI3-UTR R	ATGCTAGC TCAATCTGCC CAGTGAAATT A
cGLI3-UTR-MUT F	GCCTTATTTTGTGTTATCCTTTAACAGAGAGTTGACAAGATACGTTGACAAAT TTTCACAATGAGG
cGLI3-UTR-MUT-R	CCTCATTGTGAAAATTTGTCAACGTATCTTGTCAACTCTCTGTTAAAGGATAA CACAAAATAAGGC
c-miR-133a mimics	5'-UUGGUCCCCUUCAACCAGCUGU-3' 5'-AGCUGGUAAAAUGGAACCAAA U-3'
Sigma control siRNA	MISSION siRNA Universal negative control (#1) Sigma; product number SIC001
Gli3 MO	5'- ACGTATCTTGGTCCCTCTCTGTTAA-3'
Control MO	Standard control from GeneTools